14th Congress of the International Society of Photogrammetry, Hamburg 1980

Commission VII

Working Group VII, 4: Oceanography and Sea Ice

Invited Paper

R. C. Beal
The Johns Hopkins University
Applied Physics Laboratory
Johns Hopkins Road
Laurel, Maryland 20810

DETECTION AND TRACKING OF A LOW ENERGY SWELL SYSTEM OFF THE U.S. EAST COAST WITH THE SEASAT SAR

ABSTRACT

On the morning of 28 September 1978, at 1520 GMT, SEASAT approached the east coast of the United States, with the 100 km swath of its synthetic aperture radar (SAR) running approximately parallel to the coast, but displaced eastward by about 20 km. On the basis of the present analysis of that pass, the following major conclusions may be stated: (a) the SAR can successfully detect low-energy swell systems with significant wave heights, H_s, of well under 1 m (actually 0.65 $\pm$ 0.25 m); (b) the refraction of low-energy but well-organized swell resulting from changes in the local depth of the ocean is clearly detectable in both wavelength and direction; and (c) the complexity of the ocean spectrum (e.g., whether it is composed of more than one system or is spread in direction and wave number) seems to have little bearing on the threshold detection limits.

BACKGROUND

Studies made with aircraft in the past few years have indicated that ocean swell can be imaged with a SAR, at least for some wind velocities when there is a substantial component of the swell traveling along the radar line of sight. However, the bounds of wind, wave, and geometric conditions for which the detection of ocean waves is reliable remain elusive for want of an extensive experimental data base. SEASAT provided a unique, although limited, opportunity to re-examine the wave detection problem with few of the artificial constraints of aircraft measurements. Jordan (1978) gives a concise summary of the SEASAT SAR design parameters; Beal (1978) gives a more general description of the system and of its fundamental limitations. Preliminary assessments of its ocean wave detection capabilities have been compiled by Gonzalez (1979) and Beal (1979,1980).

During the 100 day lifetime of the SEASAT SAR, nearly 500 passes of 1 to 15 min duration were collected at three domestic and two foreign receiving stations. Twenty-three passes provided acceptable SAR imagery within 70 km of a well instrumented "sea truth" pier operated by the U.S. Army Corps of Engineers, Coastal Engineering Research Center (CERC) at Duck, North Carolina. APL and several government agencies collected wind and wave measurements from 12 August to 9 October 1978.

DISCUSSION

Figure 1 shows the areas for which estimates or measurements were collected on 28 September. For reference, the boundaries of the 100 km SAR swath are shown by the solid lines inclined approximately 25° with respect to north at this latitude. The locations are keyed alphabetically from north to south. Position A corresponds to the Navy Fleet Numerical Weather Center (FNWC) grid point 271. Positions B, C, E, and F are 15 km^2 areas over which the SEASAT SAR imagery was optically Fourier transformed. The appreciable changes in local ocean depth (dotted contours in Fig. 1) at B, C, and E would cause spreading of a single frequency deep-water wave in both wavelength and direction. Deep water dispersion prevails only at F for wavelengths greater than 70 m. Local depth changes

at B are especially severe, ranging from less than 10 to at least 20 m. The laser profilometer spectrum in Fig. 2 was collected at C by a National Oceanic and Atmospheric Administration/Sea Air Interaction Laboratory (NOAA/SAIL) aircraft. In-situ one-dimensional spectral measurements were collected at the CERC pier (D). The FNWC grid point 260 (G) provides a convenient reference spectrum for the SAR imagery data collected at F. F and G are the only deep water locations of Fig. 1.

Time histories of the long (greater than 1 s) waves were recorded by five instruments in the vicinity of the research pier for a 20 min interval spanning the satellite overpass time. The one-dimensional long-wave spectrum was measured near the pier with two Baylor gauges, two wave-rider buoys, and one capacitive wave staff. Spectra from each instrument show varying amounts of 11 and 7 s systems. The average of the two gauges and the two buoys (Fig. 2) clearly identifies each wave system. The significant wave height derived from the averaged spectrum is 1.0 m, which of course includes the combined energy from both the 11 and the 7 s systems. The significant wave height for each separate system (roughly equal in energy at the pier) is closer to 0.7 m. By comparison, the FNWC grid point closest to the pier (G) yields estimates of 0.4 and 0.6 m for the long-wave and the short-wave systems, respectively.

The NOAA aircraft flying about 50 km to the east of the pier was equipped with a laser profilometer to measure the one-dimensional ocean height spectrum in the flight direction of the aircraft. For a typical "swell-run", the aircraft heading is chosen to correspond to the vector direction of the swell (within a few degrees). The resulting spectrum accurately measures the total energy on the surface if the spectrum contains little energy orthogonal to the flight vector because that energy is effectively excluded. The laser spectrum plotted against the averaged pier spectrum in Fig. 2 verifies a double wave system with predominant periods at 11 and 7 s, and a total significant wave height of 1.26 m, or approximately 0.9 m for each system. The energy of the 7 s system is probably under-

estimated because of the directional sensitivity of the laser profilometer. However, the energy of the 11 s system should be accurate and probably represents an effective upper bound to the significant wave height in the transformed areas.

The SAR was activated for approximately four minutes on 28 September as it approached the U.S. East Coast. The radar interaction wavelength is about 30 cm, and the image intensity (or reflected power) is generally proportional to the amplitude of Bragg scatterers of the 30 cm wavelength on the ocean surface (Wright, 1968). The amplitude of the scatterers may, in turn, be strongly (but not solely) correlated with surface wind at the boundary layer. In general, brighter regions in an image correspond to higher winds and darker regions to lower winds.

The imagery from the SAR pass on 28 September was optically Fourier transformed, digitally scanned at the equivalent of 6 m ground resolution, and spatially averaged using a 7 x 7 element sliding window. The contrast was enhanced by means of a three-segment piecewise linear level transformation with a very high gain in the center segment. Each set of break points was individually optimized to compensate for the variations in average intensity.

Figure 3 shows a progression of enhanced optical Fourier transforms representing the image spectra at F, E, C, and B as the wave trains approach shore. The sequence shows quite clearly the refraction effects of the variations in ocean depth on the long-wave component. A 210 m wave in deep water at F shortens to 170 m at E, to 160 m at C, and finally to 120 m at B, in shallow water. Furthermore, the deep water spectrum of F correlates well with the FNWC estimate made at G (grid point 260) of spectral peaks in both wave number and direction. The presence of a short wave system is also evident on the transforms. This short wave energy correlation may be, at least in part, an artifact of the ground processor. Recent digitally processed and transformed imagery of the same area shows much weaker correlations in the short wave (7 s) portions of the spectrum.

It should be emphasized that no correlation between spectral energy density and image transform density has been attempted. A proper treatment of that question would require careful accounting of the many system nonlinearities, some deliberately introduced for enhancement and some unknown. A better understanding of ocean backscatter models is also a prerequisite for further progress here.

The quantitative shallow-water dispersion relationship (Kinsman, 1965) is shown by the curves in Fig. 4, on which are also plotted the results of Fig. 3. Each of the four center wavelengths from the optical transforms is entered on the horizontal axis of the dispersion relationship and is transferred according to the variation in depth for its particular location. The location of peaks from the optical transforms is judged to be accurate to $\pm 5\%$. These two uncertainties combine to produce the areas of uncertainty shown in Fig. 4. The data set is seen to be most consistent with the assumption of an 11.7 s swell system.

In summary, a well-organized, very-low-energy swell system off the east coast has been tracked with the SEASAT SAR from deep water, across the continental shelf, and into shallow water. The results indicate that a spaceborne imaging radar can measure ocean wavelength and direction accurately, even in coastal areas and in the presence of a mixed ocean. For separating swell systems in a mixed ocean, its accuracy may exceed that of any other known technique.

ACKNOWLEDGMENTS

This work was jointly supported by the National Oceanic and Atmospheric Administration and the National Aeronautics and Space Administration as a portion of the SEASAT Announcement of Opportunity Program under Contract MO-A01-78-00-4330. The laser spectrum of Fig. 2 was provided by D. Ross of NOAA. The gauge spectrum of Fig. 2 was provided by D. Lichy of CERC. J. Jenkins of APL enhanced the images shown in Fig. 3.

REFERENCES

1. R. Jordan, "The SEASAT-A Synthetic Aperture Radar Design and Implementation", Proc. Synthetic Aperture Radar Technology Conference, Las Cruces, N.M., 1978.

2. R. C. Beal, "Useful Spaceborne Synthetic Aperture Radars", Proc. XXIXth International Astronautical Federation Congress, Dubrovnik, Yugoslavia, 1978.

3. F. I. Gonzalez et al., "SEASAT Synthetic Aperture Radar: Ocean Wave Detection Capabilities", Science 204, 1979, pp. 1418-1421.

4. R. C. Beal, The SEASAT SAR Wind and Ocean Wave Monitoring Capabilities, APL/JHU S1R-79-U-019, August 1979.

5. R. C. Beal, "Spaceborne Imaging Radar Ocean Wave Monitoring", Science, Spring 1980.

6. J. W. Wright, "A New Model for Sea Clutter", IEEE Trans. Antennas and Propagation AP-16, No. 2, 1968, pp. 217-223.

7. B. Kinsman, Wind Waves, Prentice Hall, 1965, pp. 126-133.

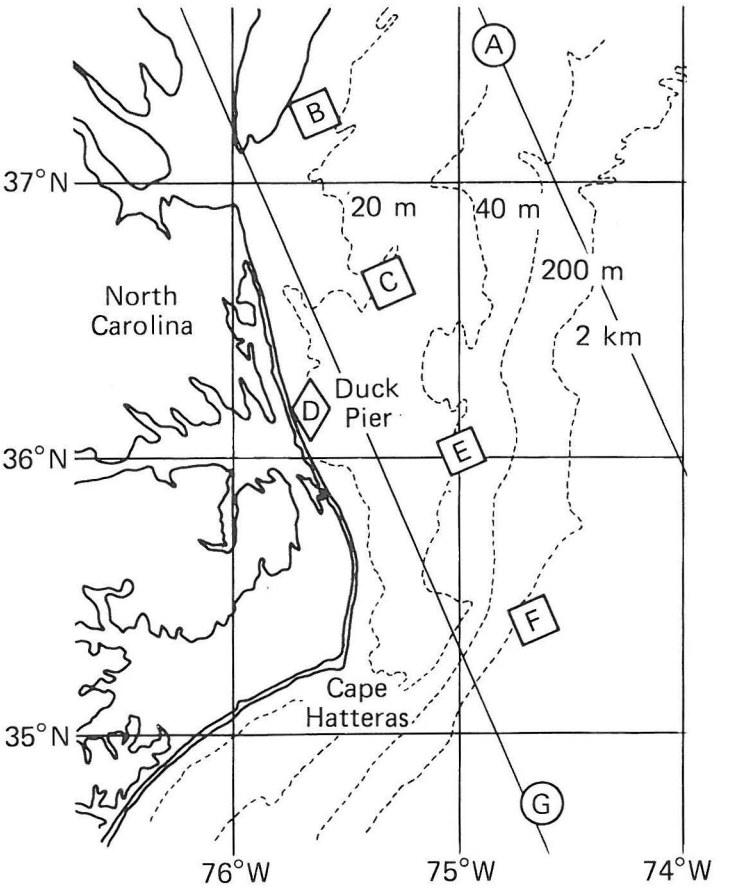

Fig. 1 Locations of surface, aircraft, and spacecraft measurements of the low-energy swell systems present on 28 September 1978.

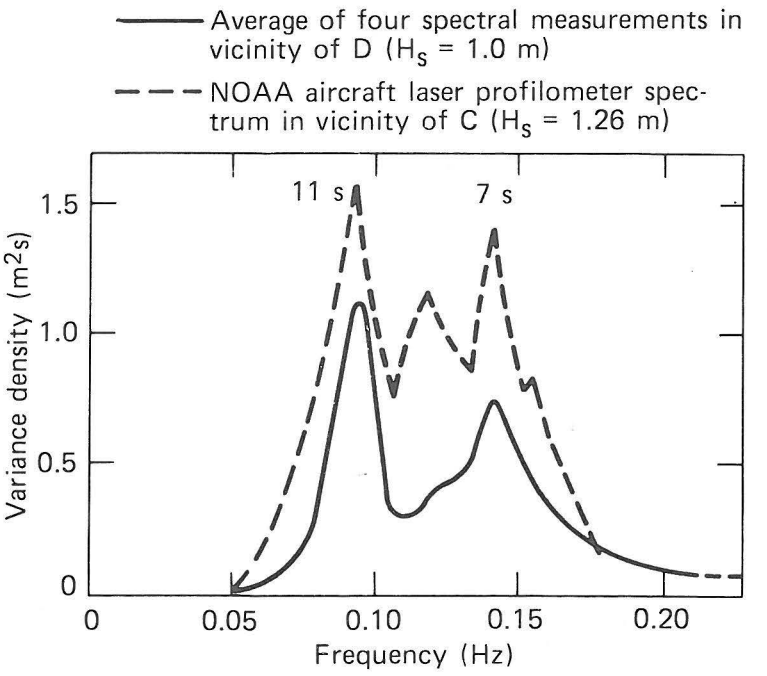

Fig. 2 A comparison of surface and air measurements of the wave height spectra near Duck, North Carolina.

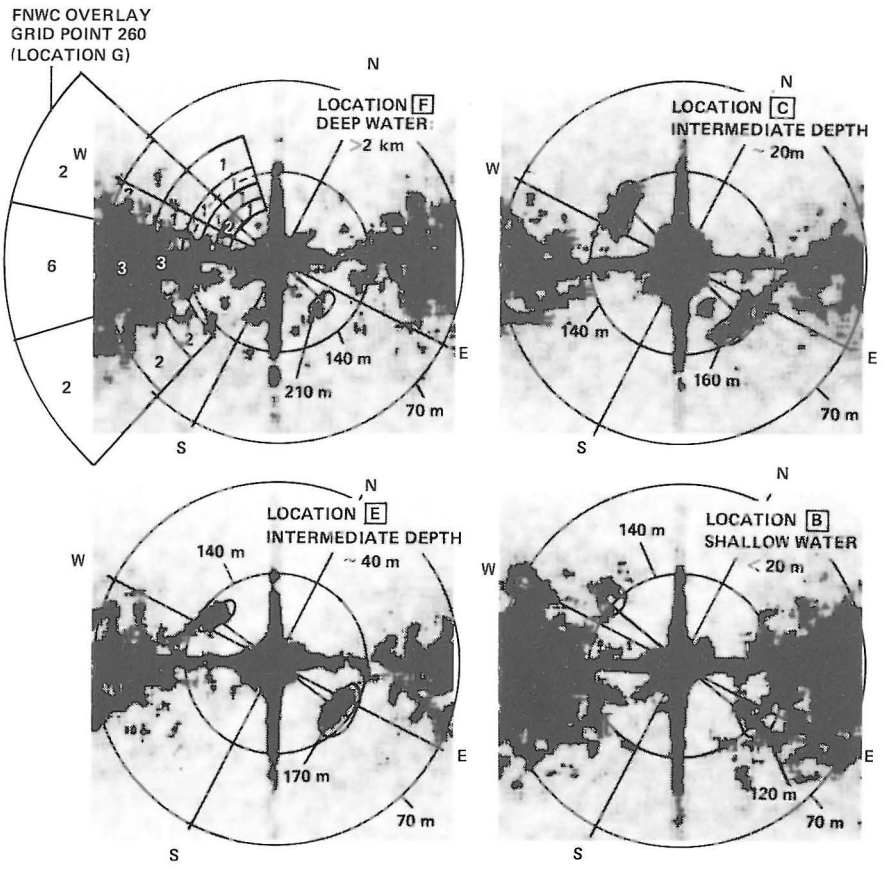

Fig. 3 Optically processed, optically transformed, and digitally enhanced SAR wave spectra from each of the four locations F, E, C, and B. The sequence moves from deep to shallow water and illustrates both wavelength and direction change as the 11 s swell system approaches shore. The overlap of the FNWC spectra for grid point 260 (G) on the SAR image spectrum at F shows excellent correlation of the 11 s swell system present on 28 September 1978. Overlay units are expressed in relative energy units per cell.

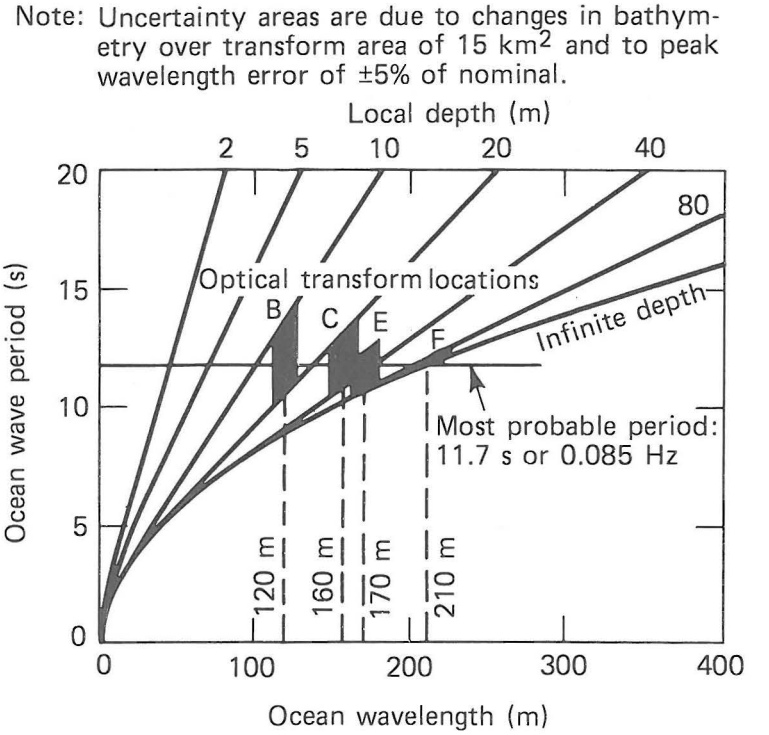

Fig. 4 The results of Fig. 3 plotted on the shallow-water dispersion relationship.